DOI: 10.12398/j.issn.2096-7217.2025.01.006

Design and testing of a liftable chassis for rice harvester

YANG Ke[1, 2], LI Ju[1, 2], CHEN Yu[1, 2], LI Hao[3], AO Yu[4], LEI Xiaolong[1, 2*]

(1. *College of Mechanical and Electrical Engineering, Sichuan Agricultural University, Ya'an* 625014, *China*; 2. *Smart Agriculture Engineering Technology Center of Sichuan Province, Ya'an* 625014, *China*; 3. *Deyang Jinxing Agricultural Machinery Manufacturing Co., Ltd, Deyang* 618000, *China*; 4. *Agriculture and Rural Bureau of Yingshan City, Nanchong* 637799, *China*)

Abstract: During the operation of the rice combine harvester, the fuselage tilts due to the tilt and unevenness of the ground affect its maneuverability and operational reliability. Aiming at the problem of leveling due to the tilt of the field surface, this research developed an innovative dual-parallelogram chassis lifting mechanism for rice harvesters designed a hydraulic system to adjust the chassis height by extending the cylinder. Using Adams simulation software, a detailed model of the lifting chassis was constructed to analyze its performance, revealing a direct correlation between the hydraulic cylinder extension and chassis elevation. Notably, the mechanism could achieve leveling on slopes with inclination angles of up to 7.5°. Comprehensive evaluations of the liftable chassis system were conducted under both static and dynamic conditions. In the static tests, the system exhibited the capacity for comprehensive or unilateral auto-leveling contingent upon the tilt, with leveling times and angular variations confined to 3.6 s and ±0.4°, respectively. In dynamic tests conducted on sloped fields and paddy soils, the system reduced post-leveling mean tilt angles and standard deviations remained below 1.2° and 0.6°, respectively. These results demonstrated a substantial improvement in the stability and reliability of the chassis during operations. This research provides valuable insights into the design and optimization of automatic leveling mechanisms and structural innovations for harvester chassis.

Keywords: rice combine harvester; chassis lifting mechanism; hydraulic leveling; leveling time

CLC number: S225.3　　**Documents code:** A　　**Article ID:** 2096-7217 (2025) 01-0059-12

YANG Ke, LI Ju, CHEN Yu, LI Hao, AO Yu, LEI Xiaolong. Design and testing of a liftable chassis forrice harvester [J]. Journal of Intelligent Agricultural Mechanization, 2025, 6(1): 59－70

阳科, 李举, 陈宇, 李浩, 敖瑜, 雷小龙. 水稻联合收获机可升降底盘的设计与试验[J]. 智能化农业装备学报(中英文), 2025, 6(1): 59－70

0　Introduction

Rice is a principal cereal crop in China, with southern regions of China characterized predominantly by hilly terrains and clayey, soft soil conditions[1]. In these challenging environments, grain combine harvesters often struggle with maneuverability, particularly in muddy fields where risks of entrapment are high. Traditional fixed chassis of harvester have deficiencies in field maneuverability and adaptability[2]. The dynamic leveling liftable chassis has become a promising solution to improve the harvester's versatility. The elevation of the chassis relative to the ground facilitates navigation and operation in deeply saturated fields[3-7]. By elevating the chassis, ground contact is optimized on uneven terrain, mitigating

Received date: 2024-07-16　　**Revised date:** 2024-08-30

Foundation item: Sichuan Science and Technology Program (2022YFG0077)

First Author: YANG Ke, Master's degree candidate, research interests: liftable chassis for rice harvester. E-mail: 2022317023@stu.sicau.edu.cn

* **Correspondence Author:** LEI Xiaolong, Doctor, Associate Professor, research interests: technology and equipment for mechanized production of rice and rapeseed. E-mail: leixl1989@163.com

damage and enhancing operational efficacy. It also curtails losses and augments travers ability. Encountering obstacles on sloped terrain is a significant hazard for agricultural machinery that predisposes it to rollover incidents[8-9]. Agricultural machinery chassis system has been focused on enhancing maneuverability, lateral stability and anti-rollover capabilities by the integration of electronic stability control, active front steering and regulators[10-16]. For example, ZHU et al.[17] developed a forestry chassis with luffing wheel legs to enhance the lateral stability, specifically when navigating forestry terrains.

Hydraulic cylinders are employed to modulate the vehicular body's angular displacement[18-19]. The design of a mechanical structure capable of autonomously adjusting its position and orientation in response to prevailing conditions is crucial[20-21]. The structural augmentation of the suspension system[22] and the integration of a control system with hydraulic components[23-24] enhance chassis leveling performance. Furthermore, sophisticated adaptive control methodologies[25], such as the QBP-PID composite algorithm-a synergistic amalgamation[26]-are deployed to continually monitor the real-time disposition of the chassis. This data-driven approach optimizes the hydraulic system's operations, ensuring precise attitude adjustments for agricultural machinery[27-30].

Although advancements in leveling systems for agricultural equipment have been made, specific research on elevation-adjustable chassis for rice harvesters remains limited. This research aims to address this gap by developing a dual-parallelogram liftable chassis for rice harvesters, designed to improve adaptability and stability on uneven and flooded terrains. The objectives are as follows: (1) to design a liftable harvester chassis capable of adjusting ground clearance and lateral tilt angle; (2) to develop a control system that harmonizes the height adjustments and tilt angles by the hydraulic cylinder chassis; (3) to evaluate the static and dynamic leveling performance of the proposed liftable harvester chassis.

1 Materials and Methods

1.1 Structure of rice harvester chassis

Figure 1 illustrates the structure of the liftable rice harvester chassis. It is primarily composed of swing arm, lifting arm, connecting rod, walking device, chassis frame, etc. The adjustment mechanism of lifting chassis operates on the principle of dual parallelogram interactions. The primary parallelogram is configured by the integration of the front lifting arm, rear lifting arm, middle beam and traveling device. Conversely, the secondary parallelogram was established through the collaboration of the front swing arm, rear swing arm, connecting rod, and chassis frame.

The lifting mechanism operated as follows: the hydraulic cylinder expanded and contracted, exerting force on the rear swing arm. This force induced rotational movement of the swing arm around the support base, altering the relative distance between the upper and lower segments of the chassis and adjusting its elevation above the ground plane. The concurrent actuation of the hydraulic cylinders in the lateral lifting mechanisms increased the total ground distance of the chassis. Selective actuation of a single hydraulic cylinder in one lifting mechanism allowed for the modulation of the chassis lateral tilt angle on that corresponding side.

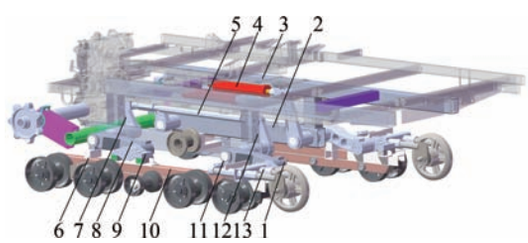


Figure 1 Structure of the lifting chassis

1. Rear lifting arm 2. Middle beam 3. Chassis frame 4. Hydraulic cylinder 5. Connecting rod 6. Limit block 7. Front swing arm 8. Front lifting arm 9. Front hinge support 10. Traveling device 11. Splined shaft 12. Rear swing arm 13. Rear hinge support

1.2 Lift chassis leveling principle

1.2.1 Lifting mechanism model analysis

Figure 2 illustrates a lifting mechanism configured such that the quadrilateral $ACDF$ forms a parallelogram. The linkage AF connects the anterior lifting arm ABC with the posterior lifting arm GED, with points C and D being affixed to the lower frame of the chassis. The hydraulic cylinder HG controls the rotation of segment GE through its extension and retraction, thereby instigating the vertical elevation of

the chassis. During the lifting process, the constancy of lengths in arms AC and DF maintain the parallelogram structural of $ACDF$. This assembly rotates about the fixed axis CD, facilitating the vertical displacement of the chassis. The parameters of each component are shown in Table 1.

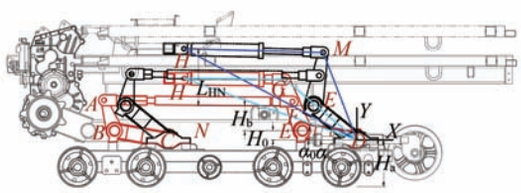


Figure 2　Liftable chassis structure schematic diagram

Table 1　Lifting mechanism parts parameters

Component	Length/mm
L_{AB}	120
L_{BC}	235
L_{DE}	235
L_{EF}	140
L_{EG}	265
L_{AF}	865
L_{GM}	610－810

Prior to the initiation of rotational motion, the angular position of segment L_{DE} was set to an initial angle of 11° ($\angle EDC$=11°). Adjustments to the chassis position were intrinsically linked to variations in its vertical elevation. This relationship was mathematically modeled as a function that describes the angular displacement of segment DE around the pivot point D (Figure 3). The mathematical correlation between the alteration in height (H_b) and the angular displacement was articulated by the ensuing trigonometric expression.

$$H_b = L_{DE} \sin \alpha \tag{1}$$

where, H_b is the lifting height of the chassis, mm; α is the angle between the swing arm DE and the chassis frame, (°); L_{DE} is the length of the rocker arm, mm.

The calculated value of H_b ranges from 0 to 140 mm. Given an initial angular deviation from 0°, the elevation angle of the swing arm at initiation is defined as follows:

$$H_0 = L_{DE} \sin \alpha_0 \approx 45 \text{ mm} \tag{2}$$

where, H_0 is initial height of chassis, mm; α_0 is the initial angle between the swing arm DE and the chassis frame, (°); L_{DE} is the length of the rocker arm, mm.

The result of H_0 is calculated as 45 mm.

A coordinate system XDY was established, with point D as the origin, the forward direction as the X-axis, and the vertical direction as the Y-axis. The relationship between the chassis ground distance (H) and the hydraulic cylinder extension length (L_{HG}) is expressed as:

$$\begin{cases} H = L_{HN} + H_a + H_b + H_0 \\ H_b = L_{BC} \sin \angle CDE \\ L_{HN} = L_{HE} \times \sin \angle HEN \end{cases} \tag{3}$$

where, L_{HN} is the vertical distance from the upper frame of the chassis to the support points of the swing arms B and E, mm; H_a is the vertical distance between the support base and the ground, mm, the result range of the chassis height H from the ground is 600-740 mm.

For operations conducted on uneven terrain, it was imperative to modulate the hydraulic cylinders on each side to adjust the tilt, thereby maintaining a horizontal working posture (Figure 3).

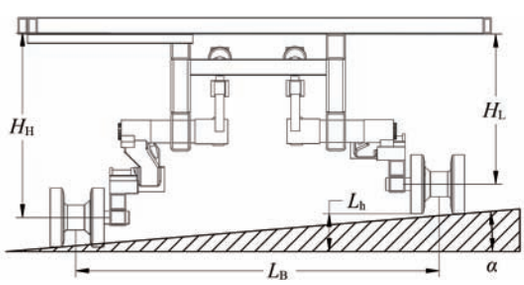


Figure 3　Analysis of tilt angle

The tilt angle of the chassis can be expressed as:

$$\alpha = \arctan \frac{H_H - H_L}{L_B} = \arctan \frac{H_b}{L_B} = \frac{L_{BC} \sin \angle CDE}{L_B} \tag{4}$$

where, α is the tilt angle of the chassis, (°); H_b is chassis lift height, mm; L_B is the distance between the left and right wheel rails, mm.

When one side of the chassis is at its highest, the maximum tilt angle is 7.2°.

The relationship between the rotation angle (θ) of the rocker arm (EG) and the extension length of the hydraulic cylinder can be expressed as follows:

$$\theta = \arccos \frac{L_{EH}^2 + L_{EM}^2 - (L_{HG} + \Delta s)^2}{2 \cdot L_{EH} \cdot L_{EM}} - \arccos \frac{L_{EH}^2 + L_{EG}^2 - L_{HG}^2}{2 \cdot L_{EH} \cdot L_{EG}} \tag{5}$$

where, M is the extended position of point G of the hydraulic cylinder head, mm.

The calculated value range of θ is 29°.

1.2.2 Leveling method analysis

The adjustment of harvester chassis primarily involved two axes: X and Y. The plane $A_0B_0C_0D_0$ can be derived by rotating plane $A_2B_2C_2D_2$ about the Y by an angle of β degrees (Figure 4).

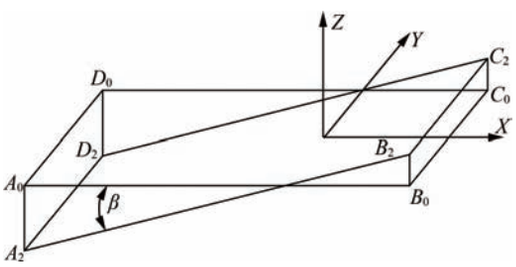


Figure 4 Schematic diagram of chassis rotation coordinates

In an inclined plane, a point designated as P_1 with coordinates (x_1, y_1, z_1) was subjected to a β-degree rotation about the Y-axis, yielding transformed coordinates (x, y, z). The corresponding rotation matrix for this transformation is denoted as:

$$R=\begin{bmatrix}x\\y\\z\end{bmatrix}=\begin{bmatrix}\cos\beta & 0 & \sin\beta\\0 & 1 & 0\\-\sin\beta & 0 & \cos\beta\end{bmatrix}\begin{bmatrix}x_1\\y_1\\z_1\end{bmatrix} \tag{6}$$

$$\begin{bmatrix}x\\y\\z\end{bmatrix}=\begin{bmatrix}\cos\beta & 0 & \sin\beta\\0 & 1 & 0\\-\sin\beta & 0 & \cos\beta\end{bmatrix}\begin{bmatrix}x_1\\y_1\\z_1\end{bmatrix} \tag{7}$$

Upon assuming $\sin\beta=\beta$ and $\cos\beta=1$, these approximations can be integrated into Equation 8. Consequently, the correlation between support points and inclination angles is as follows:

$$\begin{bmatrix}x\\y\\z\end{bmatrix}=\begin{bmatrix}1 & 0 & \beta\\0 & 1 & -\alpha\\-\beta & \alpha & 1\end{bmatrix}\begin{bmatrix}x_1\\y_1\\z_1\end{bmatrix} \tag{8}$$

The coordinates for the four supporting points were designated as follows: Point A_0 was located at the origin (0, 0, 0), Point B_0 was positioned at (a, 0, 0) along the positive X-axis, Point C_0 was situated in the first quadrant of the XY-plane at (a, b, 0), and Point D_0 was placed along the positive Y-axis at (0, b, 0).

$$\begin{bmatrix}A_0\\B_0\\C_0\\D_0\end{bmatrix}^T=\begin{bmatrix}0 & 0 & a & a\\0 & b & 0 & b\\0 & 0 & -\beta a & -\beta a\end{bmatrix} \tag{9}$$

Figure 4 depicts points B_0 and C_0 as the apices, indicating that these points remain stationary while rotation occurs at the other two points. The elevations attained by these rotating points are recorded as follows:

$$\begin{cases}A_0=0\\B_0=-\beta a\\C_0=-\beta a\\D_0=0\end{cases} \tag{10}$$

where, a is the length along the X-axis, mm; b is length along the Y-axis, mm.

1.2.3 Stability analysis of the liftable chassis

Figure 5 illustrates the force analysis of a rice harvester chassis during lateral inclination, with the tracks on each side acting as fulcrums. As one side descends, the harvester center of mass translates horizontally to the left, indicated by the distance L_{OO_1}.

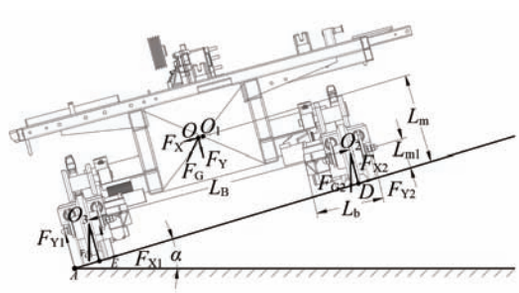


Figure 5 Lateral tilt centroid analysis

Upon inclination of the harvester chassis, stress becomes concentrated at point E. The static equilibrium equation for point E can be articulated as follows:

$$\sum M_E=0 \tag{11}$$

$$F_{Y1}\cdot L_B+F_X\sin\alpha\cdot L_m-F_Y\cos\alpha\left(\frac{1}{2}L_B-L_{OO_1}\right)=0 \tag{12}$$

where, L_B is the left and right wheel-rail gauge, mm; m is height of center of gravity of rice harvester, mm; L_{OO1} is center of gravity offset during roll, mm.

The lateral force F_{Y1} is expressed as:

$$F_{Y1}=\frac{F_X\sin\alpha\cdot L_m-F_Y\cos\alpha\left(\frac{1}{2}L_B-L_{OO_1}\right)}{L_B} \tag{13}$$

The initiation of chassis rollover is determined by two primary conditions: the cancellation of the lateral force component (F_{Y1}=0) and the removal of the eccentricity between the vehicle's center of gravity (O) and the application point of the resultant force (O_1). The maximum roll angle is as follows:

$$\alpha_{max}=\arctan\frac{L_B}{2L_{h1}}=30.4^\circ \tag{14}$$

where, α_{max} is maximum roll angle, (°); L_B is the left

and right wheel-rail gauge, mm; L_{h1} is height of center of mass, mm.

The calculation shows that the maximum lateral stability limit slope of the harvester is 30.4°.

1.3 3D model and simulation

1.3.1 ADAMS kinematics simulation

A three-dimensional model of the liftable chassis for a rice harvester was developed in SolidWorks, and imported into the ADAMS simulation environment for kinematic and stress analysis (Figure 6). Within ADAMS, constraints and interconnections were applied in accordance with actual operational conditions, with the lifting mechanism connected to a hydraulic cylinder via a pin shaft. The model consists of 16 revolute joints, 2 translational joints, 2 fixed joints, 2 planar joints, and 2 cylindrical joints.

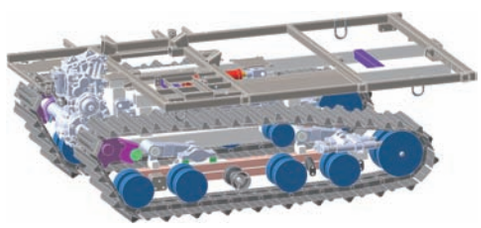


Figure 6 Lifting chassis model

To accurately simulate agricultural field conditions, the chassis was subjected to comprehensive load analysis under various structural configurations for detailed stress evaluation. The assignment of mass properties involved determining the mass, centroid location, and moments of inertia, etc. The rice combine harvester, with a tare weight of 2 210 kg and a grain tank capacity of roughly 1 cubic meter. was analyzed considering the density of rice at approximately 0.75 tons per cubic meter, resulting in a total mass was about 3 tons.

1.3.2 Lifting mechanism hydraulic drive parameters

The driving parameters of the hydraulic cylinders were established based on 2 scenarios, the overall lifting and unilateral lifting of the chassis. The expansion range of the hydraulic cylinder was set 0-175 mm. When the chassis was lifted, the driving parameters of the hydraulic cylinder were simulated and analyzed. The elevation mechanism of the chassis was predominantly influenced by two actuation paradigms: activation of the left hydraulic cylinder induces elevation on the chassis left side, whereas the right hydraulic cylinder regulates elevation on the right side. The concurrent operation of both cylinders ensured homogeneous elevation of the entire chassis. In ADAMS, a driver was incorporated into the hydraulic cylinder motion pair. This driver utilized the step function as its driving parameter. The function format is:

$$STEP(x, x_0, h_0, x_1, h_1) \tag{15}$$

where x is independent variable; x_0 is starting point, s; h_0 is initial function value, mm; x_1 is end point, s; h_1 is Final function value, mm.

The driving function of the left hydraulic cylinder was: *STEP* (time, 0, 0, 15, 175) + *STEP* (time, 15, 0, 20, −100) + *STEP* (time, 20, 0, 30, −175); The driving function of the right hydraulic cylinder was: *STEP* (time, 0, 0, 15, 175) + *STEP* (time, 15, 0, 20, −100) +*STEP* (time, 20, 0, 30, −175).

1.4 Development of hydraulic system

The hydraulic system comprised a filter, a proportional directional valve, a non-return valve, a pressure sensor, two magnetic displacement sensors, a hydraulic cylinder, two balance valves, and two three-position four-way solenoid valves (Figure 7). The balance valve regulated the descending speed, while the solenoid valve controlled the initiation, termination, and direction of the hydraulic cylinder motion. An angle sensor was employed to detect the chassis inclination angle, a pressure sensor indicating the hydraulic pressure, and magnetic displacement sensors measuring the cylinder extension and retraction.

Upon detection of chassis inclination by the inclination sensor, the hydraulic system was activated, prompting the electromagnetic control valve to adjust accordingly. This engagement either extended or contracted the hydraulic cylinder, thereby driving the lifting mechanism to vertically adjust the chassis. Concurrently, the proportional flow valve was operated to ensure that the flow rate of the hydraulic cylinder remained within an appropriate range. By controlling the speed of extension and contraction of the hydraulic cylinder, the system response time and leveling precision can be regulated. The balance valve provided pressure compensation by adjusting the pressure differential, While the integrated displacement sensor continuously monitored the cylinder position, which

provided feedback to the control system for closed-loop adjustment. This enhanced the system operational accuracy and efficiency (Figure 8).

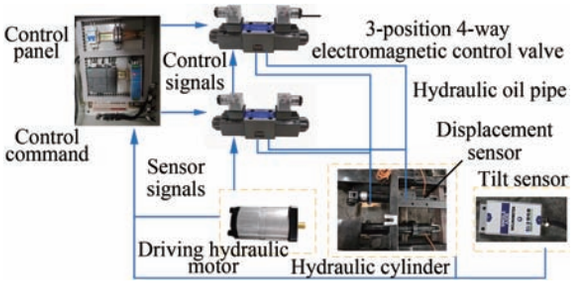


Figure 7 The structure of the hydraulic control system

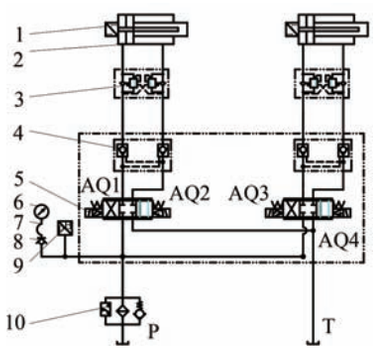
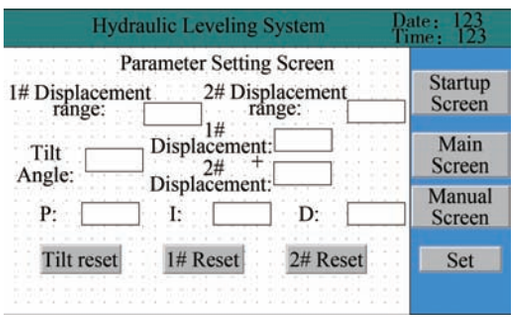


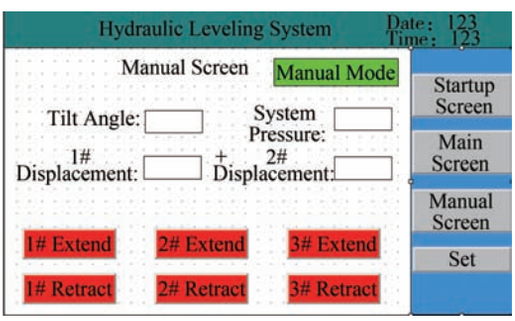
Figure 8 Hydraulic control schematic diagram.

1. Hydraulic cylinder 2. Magnetic displacement sensor
3. Two-way balancing valve 4. Hydraulic lock (one-way valve)
5. Proportional directional valve 6. Shock-resistant pressure gauge
7. Pressure measuring hose 8. Pressure measuring joint
9. Pressure sensor 10. High-pressure filter

The automatic lifting electro-hydraulic control system includes a displacement sensor, an angle sensor, an oil pressure sensor, a controller, a display and an operating handle. The controller is based on Siemens SR20-PLC[31], with the hydraulic cylinder control mechanism governed by an S7-200 Programmable Logic Controller (PLC) as the central command module. The proportional valve digital signals are transformed into analog format via the AM06 module, while the AM04 module performs analog-to-digital conversion for data from displacement and inclination sensors. The converted data is processed by the CPU ST20 and subsequently executed by the pertinent units. The hydraulic system features a human-machine interface equipped with a touchscreen that displays pivotal parameters such as tilt angle, pressure, cylinder stroke, and valve output (Figure 9). This interface supports two modes of chassis leveling: automatic and manual. The hydraulic leveling system primarily employs a proportional-integral-derivative (PID) control algorithm to compute the control volume for hydraulic cylinder extension and retraction based on the system error signal. This process ensures precise adjustment ofthe output of the leveling system, enabling the hydraulic control system to achieve rapid response time and minimal overshoot in adjusting the tilt angle of the fuselage (Figure 9).



(a) Main interface of hydraulic control system



(b) Manual and automatic operation interface of hydraulic control system

Figure 9 Hydraulic system interface

1.5 Test method

Static and field experiments were conducted to verify the accuracy and stability of the liftable chassis in at the Teaching and Research Center of the Ya′an Campus of Sichuan Agricultural University (Figure 10) and Bangfu Professional Cooperative, Jianping Town, Santai County, Sichuan Province, under no-load conditions to validate the functional implementation of the lifting chassis and assess its lifting speed, hydraulic system response time, and lifting effect in the absence of external load.



Figure 10 Rice harvester with integrated lifting system

1.5.1　Static experiments

The static test was conducted to verify the feasibility of the liftable chassis balance system of rice combine harvester. The inclination angle and displacement of the hydraulic cylinder were measured using a Vit WT901BLE inclinometer and displacement sensor, which was connected to a computer to establish an upper-level data acquisition system for collecting data on the extension and retraction of the hydraulic cylinder and the inclination angle.

The static experiment consists of three parts: (1) placing one side of the chassis at the lowest point while elevating the opposite side to generate specific tilt angles, then activating the automatic leveling switch and recording the leveling process; (2) placing the chassis at its lowest height, lifting both sides simultaneously to establish the correlation between the vertical displacement of the chassis and the extension and retraction of the hydraulic cylinder; (3) fixing one side of the chassis and lifting the opposite sideto measure and record the lateral inclination angle of the chassis and the rotation angle of the rotating arm.

The relationship between the lifted height of the chassis and the extension and retraction of the hydraulic cylinder was established. The tilt angles were set as 1.5°, 5° and 8° and each test was repeated three times.

1.5.2　Dynamic experiments

The dynamic experiments included slope tests and paddy field tests, designed to verify accuracy and stability of the liftable chassis control.

1) The slope test, conducted on an incline with angles ranging from 2° to 12° and height differences between 10 to 20 cm, evaluated the automatic leveling system of a rice combine harvester. During the test, the harvester chassis was driven along a hilly slope without activating the automatic mode, and its tilt data was captured using an inclination sensor. The test was then repeated with the automatic leveling feature engaged, and its tilt data was recorded again. A comparative analysis of the tilt data, both with and without the automatic leveling function, was performed to assess the effectiveness of the automatic leveling under consistent operating conditions.

2) The paddy field test was conducted in a single paddy field at 3 speeds: 1 km/h, 1.8 km/h, and 2.5 km/h. These tests involved circumnavigating the field perimeters while performing leveling assessments and conducting control experiments by activating and deactivating automatic leveling features. The study meticulously analyzed the duration of leveling when operated automatically and the subsequent alterations in the tilt angles. A comparative analysis was then employed to discern the efficacy of automatic leveling versus manual adjustments under identical operational conditions.

2　Results and discussion

2.1　Results of simulation analysis

Figure 11 illustrates the displacement profiles of the left and right hydraulic cylinders during the simulation.

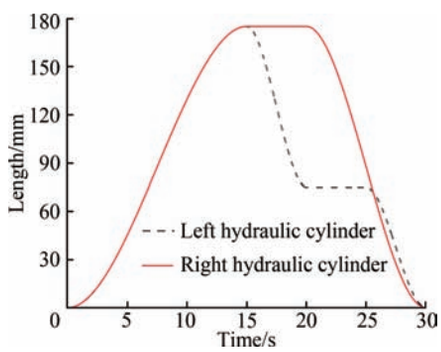


Figure 11　Hydraulic cylinder extension length

In the first 15 s, the left cylinder extended by 175 mm. From 15 to 20 s, the left cylinder contracted by 100 mm while the right maintained its position, causing an elevated left side and a lowered right side of the chassis. The left cylinder was stationary from 20 to 25 s as the right retracted by 100 mm, leveling the chassis by 25 s.

Finally, both cylinders descended synchronously by 75 mm from 25 to 30 s, returning to their initial positions. This demonstrates precise control over the cylinders movements.

The relationship between the chassis inclination angle and the extension lengths of the left and right hydraulic cylinders is presented in Figure 12, from which a mathematical formula correlating the inclination angle with the extensions of the hydraulic cylinders was derived.

The peak rotational displacement of the chassis

lifting mechanism was 7.40° on the right side and 7.46° on the left, resulting in a lateral tilt angle fluctuation between −7.40° and +7.46° (Figure 13).

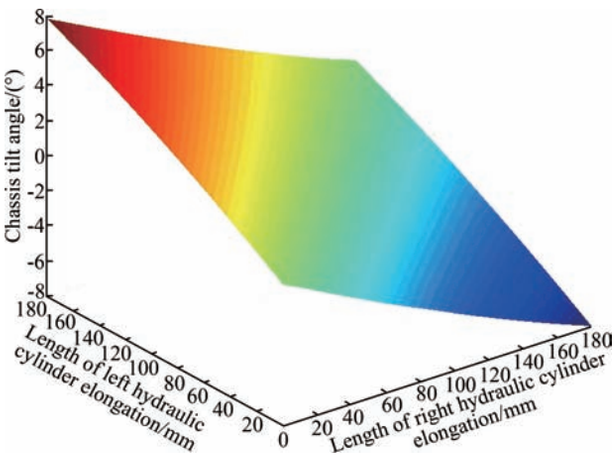


Figure 12 Relationship between chassis inclination angle and hydraulic cylinder extension length

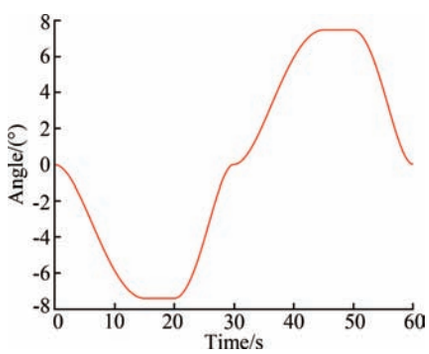
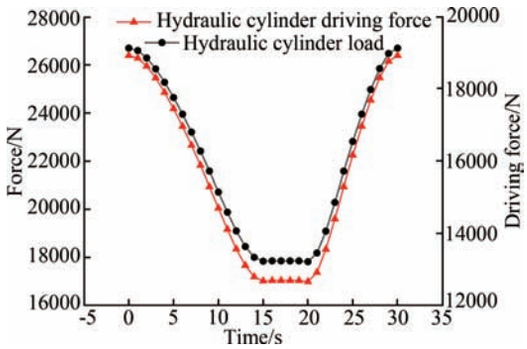


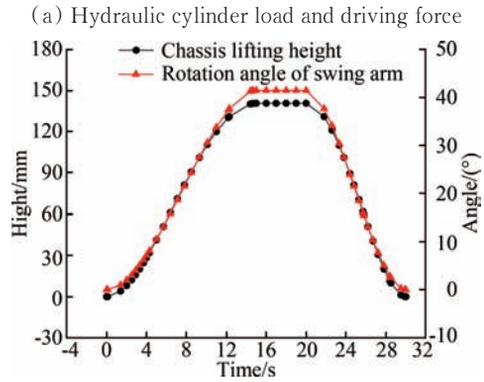
Figure 13 Chassis lateral tilt angle

Figure 14 illustrates that the hydraulic cylinder reached its maximum force of 26 714.65 N at 0.1 s, with a peak driving force of 18 963.38 N, indicating significant force application during the initial lifting of the chassis. Between 0 to 15 s, as the cylinder extended, there was a gradual reduction in force and an increase in the rotation angle of the rocker arm. From 15 to 20 s, the swing arm achieved its maximum rotation of 42°, the cylinder extended by 175 mm, the chassis height was increased by 150 mm, and the driving force stabilized at 12 635.63 N, while the experienced force diminished to a minimum of 17 812.87 N. Between 20 to 35 s, the retraction of the cylinder resulted in its shortening and a decrease in the swing arm rotation angle, causing a progressive increase in both force and driving force, reaching maxima upon returning to the initial position.

This symmetrical loading and actuation confirmed that hydraulic action effectively modulated the rotation of the swing arm through cylinder extension and retraction, thereby adjusting chassis height.



(a) Hydraulic cylinder load and driving force



(b) Chassis lift height and arm angle

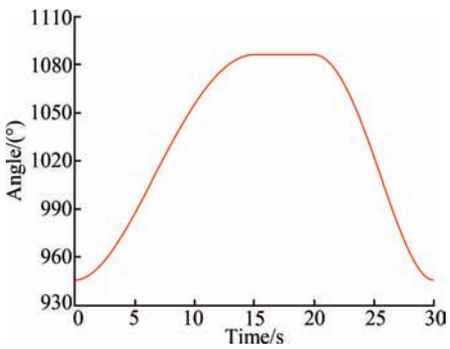
Figure 14 Lifting height and force of lifting chassis

The hydraulic cylinder extension elevated the chassis, increasing its height and shifting the center of mass from 946.63 mm to 1 086.27 mm, a displacement of 140.64 mm, as shown in Figure 15(a). This shift indicated a significant change in the chassis dynamics. The impact force could be inferred from the acceleration of the center of mass, which peaked at 11.05 mm/s^2 after 20 s. Concurrently, the center of mass velocity reached a maximum of 25.04 mm/s at 24.8 s, as illustrated in Figure 15(b). This indicates that the chassis underwent significant acceleration during lifting and stopping, potentially causing larger impact force.

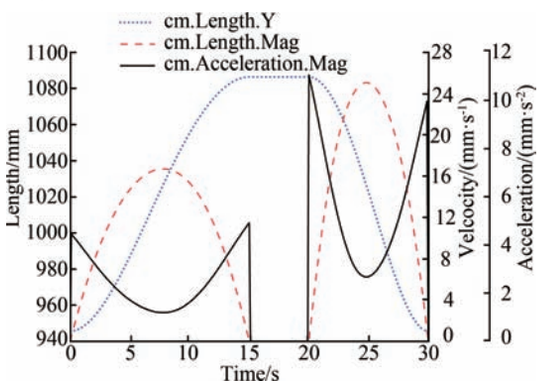
2.2 Results of the static test

The results of the static tests of the liftable chassis at tilt angles of 1.5°, 5°, 8° are shown in Figure 16. These results demonstrate the chassis rapid leveling capability when subjected to inclination status. Initial angles were 8.1°, 5.05°, 1.24°, −1.17°, −4.70°, and −7.52°. After leveling, the angles were corrected to 0.15°, 0.10°, −0.08°, −0.35°, −0.22°, and −0.1°, with corresponding adjustment times of 2.72 s, 2.32 s, 3.52 s, 2.92 s, 2.20 s, and 2.62 s,

respectively. Notably, the overall adjustment errors remained below 0.4°, and the mean adjustment time was less than 3.60 s. This shows that the automatic chassis leveling system operated robustly, efficiently calibrating various chassis inclinations to a level state expeditiously.



(a) Height of the center of mass in the Y direction of the harvester



(b) Center of mass velocity and acceleration

Figure 15　Center of mass height, velocity and acceleration

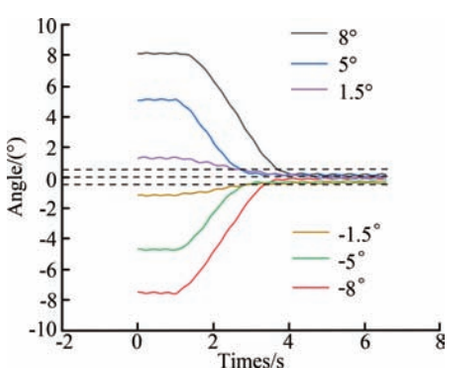


Figure 16　Tilt statue in the static test

As illustrated in Figure 17, the initial ground clearance of the chassis was 255 mm with a rocker arm angle of 11°. As the hydraulic cylinder extended, the rocker arm rotated, elevating the chassis. At 175 mm cylinder extension, the chassis clearance increased to 393 mm, an elevation gain of 138 mm. The extension of the hydraulic cylinder facilitated the rotation of the lever arm, showcasing a linear relationship between the chassis elevation, the rotation angle of the swing arm, and the extension of the hydraulic cylinder. This indicates that precise control over the extension of the hydraulic cylinder can achieve adjustments in the overall lifting and tilting states of the chassis, enhancing its adaptability and stability.

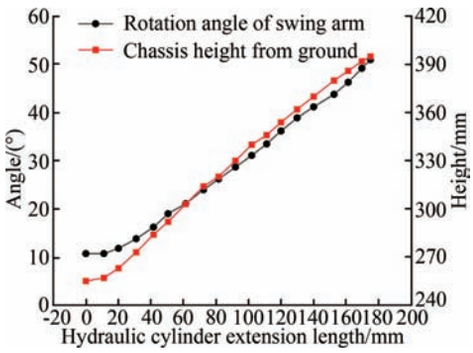


Figure 17　Relationship between extension length of hydraulic cylinder, rotation angle and lifting height

Figure 18 illustrates the lateral inclination, classified into left and right chassis tilts. During the assessment of left-tilt, a peak angle of 7.41° was attained when the hydraulic cylinder was extended to 175 mm. Similarly, in the evaluation of right-tilt, a maximum angle of 7.55° was realized at the same cylinder extension. These results indicate that the chassis lateral tilt capacity is approximately 7.5°.

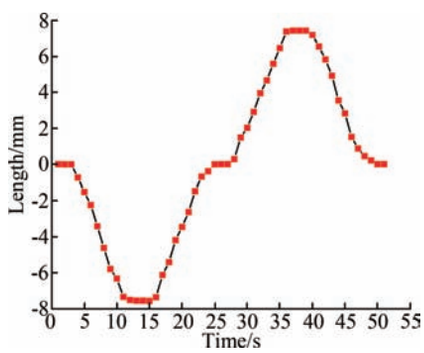


Figure 18　Chassis lateral tilt angle

2.3　Results of dynamic leveling test

The efficacy of the leveling system on sloped terrain was shown in Figure 19. When the system was not activated, the harvester's chassis oscillated between −12° and 11.2° while traversing an uneven groove, indicating substantial terrain variability. Upon enabling the automatic leveling function, acute chassis tilting occurred as the track encountered significant elevation differences, prompting the system to issue a leveling command that mitigated the inclination angle. The

leveling system demonstrated a significant reductionin both mean and standard deviation of the tilt angle compared to non-leveling conditions, with the mean changing from 7.38° to 0.99° and the variance changing from 56.33% to 6.21%, quantified by a notable percentage decrease. Consequently, the system can effectively level the chassis within 2 to 3 s when confronts slope-induced tilt, thereby enhancing stability and reliability.

The results of the automatic leveling of liftable chassis at different speeds in the paddy field were further analyzed (Figure 20). It indicated that for all tested speeds, both the mean and standard deviation of the tilt angle were significantly lower when the automatic leveling mode was active compared to operation without leveling. During operation in auto-level mode, while there was an increase in the average leveling angle with an increase in travelling speed, it consistently remained under 1.2°. The standard deviation was consistently low, not surpassing 0.6°, suggesting that the adjustable chassis sustained robust stability and reliability under different travelling speeds.

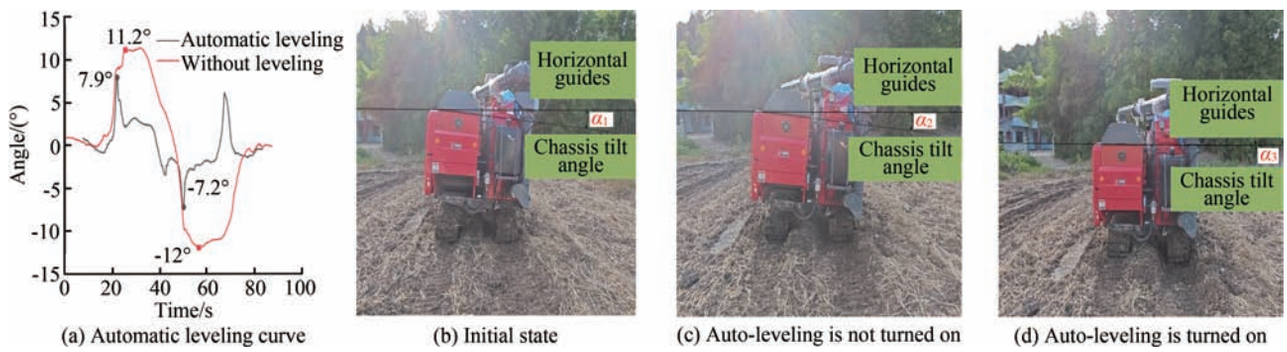


Figure 19 Automatic leveling test of pothole fields

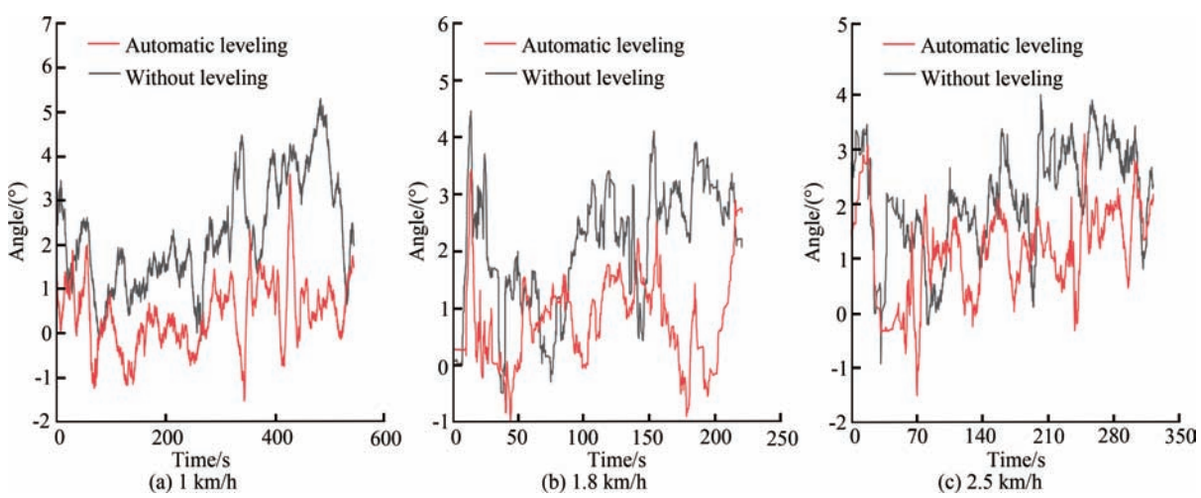


Figure 20 Automatic leveling of field tests at different travelling speeds

Table 2 Field test results

Travelling speed/(km·h^{-1})	Average leveling angle/(°)		Standard deviation of leveling angle/(°)	
	Automatic leveling	Without leveling	Automatic leveling	Without leveling
1.0	0.46	2.24	0.58	1.48
1.8	0.92	2.11	0.53	0.89
2.5	1.18	2.00	0.55	1.02

3 Conclusions

This study presented a liftable chassis leveling system for a rice combine harvester. The lifting mechanism of the chassis was designed using a four-bar mechanism. The conclusions were as follows:

1) A theoretical analysis was undertaken to develop a dual parallelogram lifting mechanism for a rice harvester

chassis, followed by the design of a hydraulic system to actuate the chassis elevation using hydraulic cylinders. A simulation model of the lift mechanism was established by Adams software, and kinematic analyses. Results showed a direct linear correlation between the hydraulic cylinder stroke and the chassis elevation, facilitating leveling on an inclination angle of 7.5°.

2) Static tests confirmed the system ability to auto-level according to tilt angle, allowing full elevation and unilateral leveling adjustments with overall errors of 0.4° and an average adjustment time under 3.60 s.

3) Dynamic leveling tests on slopes and in paddy fields ascertained that the automated leveling system significantly improved the chassis tilt, thereby enhancing stability. The automatic leveling system consistently maintained post-leveling average tilt angles and standard deviations below 1.2° and 0.6° respectively. This research concludes that the implemented automatic chassis elevation system substantially improves the stability and reliability of the rice harvester chassis in challenging terrains such as slopes and paddy fields.

References

[1] WEI Zhongcai, WANG Xinghuan, LI Xueqiang, et al. Design and experiment of crawler self-propelled sorting type potato harvester [J]. Transactions of the Chinese Society of Agricultural Machinery, 2023, 54(2): 95−106.

[2] JIN Chengqian, YANG Tengxiang, LIU Gangwei, et al. Design and test of posture controlled chassis for caterpillar combine [J]. Transactions of the Chinese Society for Agricultural Machinery, 2020, 51(11): 393−402.

[3] SUN Yixin, XU Lizhang, JING Bo, et al. Development of a four-point adjustable lifting crawler chassis and experiments in a combine harvester [J]. Computers and Electronics in Agriculture, 2020, 173.

[4] HU Jinpeng, PAN Jiahui, DAI Buwang, et al. Development of an attitude adjustment crawler chassis for combine harvester and experiment of adaptive leveling system [J]. Agronomy, 2022, 12(3): 717−717.

[5] SUN Jingbin, MENG Chong, ZHANG Yazhou, et al. Design and physical model experiment of an attitude adjustment device for a crawler tractor in hilly and mountainous regions [J]. Information Processing in Agriculture, 2020, 7(3): 466−478.

[6] JING Bo, XU Lizhang. Design and simulation of liftable crawler chassis for combine harvester [J]. Journal of Advances in Agriculture, 2018, 8: 1476−1487.

[7] GUAN Zhuohuai, ZHANG Min, JIN Mei, et al. Research progress of mechanical damage to soil by walking mechanism of tracked agricultural equipment [J]. Journal of Intelligent Agricultural Mechanization, 2022, 3(1): 62−70.

[8] JANG M K, HWANG S J, KIM J H, et al. Overturning and rollover characteristics of a tractor through dynamic simulations: Effect of slope angle and obstacles on a hard surface [J]. Biosystems Engineering, 2022, 219: 11−24.

[9] RONDELLI V, CASAZZA C, MARTELLI R. Tractor rollover fatalities, analyzing accident scenario [J]. Journal of safety research, 2018, 67: 99−106.

[10] LI Z, MITSUOKA M, INOUE E, et al. Parameter sensitivity for tractor lateral stability against Phase I overturn on random road surfaces [J]. Biosystems engineering, 2016, 150: 10−23.

[11] SONG Y, ZHANG X, WANG W. Rollover dynamics modelling and analysis of self-propelled combine harvester [J]. Biosystems Engineering, 2021, 209: 271−281.

[12] YOON J, CHO W, KANG J, et al. Design and evaluation of a unified chassis control system for rollover prevention and vehicle stability improvement on a virtual test track [J]. Control Engineering Practice, 2010, 18(6): 585−597.

[13] VERMILLION C, SUN J, BUTTS K. Modeling, control design, and experimental validation of an overactuated thermal management system for engine dynamometer applications [J]. IEEE transactions on control systems technology, 2008, 17(3): 540−551.

[14] BADGUJAR C, FLIPPO D, WELCH S. Artificial neural network to predict traction performance of autonomous ground vehicle on a sloped soil bin and uncertainty analysis [J]. Computers and Electronics in Agriculture, 2022, 196: 106867.

[15] FRANCESCHETTI B, RONDELLI V, CIUFFOLI A. Comparing the influence of Roll-Over protective structure type on tractor lateral stability [J]. Safety science, 2019, 115: 42−50.

[16] AHMADI I. Dynamics of tractor lateral overturn on slopes under the influence of position disturbances (model development) [J]. Journal of Terramechanics, 2011, 48(5): 339−346.

[17] ZHU Y, KAN J. Prediction of the lateral stability of a forestry chassis with an articulated body and fitted with luffing wheel-legs [J]. Biosystems Engineering, 2022, 224: 143−160.

[18] HAS Z, RAHMAT M F, HUSAIN A R, et al. Robust position tracking control of an electro-hydraulic actuator in the presence of friction and internal leakage [J]. Arabian Journal for Science and Engineering, 2014, 39: 2965−2978.

[19] ZHANG Zhaoguo, WANG Yichi, LI Hanqing, et al. Design and test of hydraulic control tracked self-propelled greenhouse panax notoginseng harvester [J]. Transactions of the Chinese Society of Agricultural Machinery 2021, 52(6): 127－135, 158.

[20] JIAO X, XIE J, WANG X, et al. Intelligent decision method for the position and attitude self-adjustment of hydraulic support groups driven by a digital twin system [J]. Measurement, 2022, 202: 111722.

[21] GE X, XIE J, WANG X, et al. A virtual adjustment method and experimental study of the support attitude of hydraulic support groups in propulsion state [J]. Measurement, 2020, 158: 107743.

[22] HU L, GAO H, LIU Z, et al. Configuration design and kinematic performance analysis of a parallel wheelset suspension for a multi-wheeled pressurized lunar rover [J]. Acta Astronautica, 2024, 217: 162－180.

[23] DETTÙ F, CORNO M, D′AMBROSIO D, et al. Modeling, control design and experimental automatic calibration of a leveling system for combine harvesters [J]. Control Engineering Practice, 2023, 132: 105411.

[24] DU Xiaoqiang, NING Chen, YANG Zhenhua, et al. Design and experiment of hydraulic system for crawler chassis of straddle type camellia oleifera fruit harvester [J]. Transactions of the Chinese Society of Agricultural Machinery 2023, 54(3): 139－147.

[25] SUN Xiaoqiang, CAI Yignfeng, YUAN Chaochun, et al. Fuzzy sliding mode control for the vehicle height and leveling adjustment system of an electronic air suspension [J]. Chinese Journal of Mechanical Engineering, 2018, 31(2): 238－250.

[26] JIANG Y, SUN Z, WANG R, et al. Design and control of a new omnidirectional levelling system for hilly crawler work machines [J]. Computers and Electronics in Agriculture, 2024, 218: 108661.

[27] FENG Y, TIAN X, LI T, et al. Measurement of mobile manipulator chassis pose change caused by suspension deformation and end-effector accuracy improvement based on multi-sensor fusion [J]. Robotics and Autonomous Systems, 2023, 170: 104553.

[28] ZHAO Zhiyu, ZHU Licheng, ZHOU Liming, et al. Design and experiment of chassis control system for weeding robot in hilly orchard [J]. Transactions of the Chinese Society for Agricultural Machinery, 2022, 53, 48－57.

[29] ZHAO Weisong, CHEN Yongsheng, WANG Zhenwei, et al. Design and experimental verification of conveying device for crushed cornstalks [J]. Journal of Intelligent Agricultural Mechanization (in Chinese and English), 2021, 2(1): 1－12.

[30] ZHU Zhengbo, CAO Xin, ZHANG Ruihong. Optimal design of garlic clove′s orientation adjustment system based on parallel robot [J]. Journal of Intelligent Agricultural Mechanization, 2023, 4(4): 20－25.

[31] LEI Xiaolong, CHEN Yu, YANG Ke, et al. Design and experiment of chassis automatic lifting hydraulic system for harvester [J]. Journal of Intelligent Agricultural Mechanization, 2024, 5(2): 9－18.

水稻联合收获机可升降底盘的设计与试验

阳科[1, 2]，李举[1, 2]，陈宇[1, 2]，李浩[3]，敖瑜[4]，雷小龙[1, 2*]

（1. 四川农业大学机电学院，四川雅安，625014；2. 四川省智慧农业工程技术研究中心，四川雅安，625014；3. 德阳金星农业机械制造有限公司，四川德阳，618000；4. 四川省营山市农业农村局，四川南充，637799）

摘要：水稻联合收割机在作业过程中由于地面倾斜和不平整导致机身倾斜，影响其通过性和可靠性。本研究针对田间表面倾斜需要调平的问题，设计了一种适用于水稻联合收获机的双平行四边形底盘升降机构，并设计了液压系统，通过油缸伸出实现对底盘高度的调整。利用Adams软件构建了升降底盘的仿真模型，分析得出液压缸伸出长度与底盘高度呈正相关关系，且该机构能够在7.5°的倾斜角度下实现调平；并对可升降底盘系统进行了静态和动态评价。在静态试验中，系统能够根据倾斜情况实现全面或单侧自动调平，调平时间和角度偏差分别控制在3.6 s和±0.4°以内。在斜坡地和水田地上的动态测试显示，调平后的平均倾斜角度和标准差分别保持在1.2°和0.6°以下，显著提高了底盘的稳定性和可靠性。本研究为水稻联合收获机底盘的自动调平技术和结构设计提供了参考。

关键词：水稻联合收割机；底盘升降机构；液压调平；调平时间